Published in final edited form as:
Nat Med. 2014 January ; 20(1): . doi:10.1038/nm.3416.

Magnetic resonance imaging of tumor glycolysis using hyperpolarized ^{13}C-labeled glucose

Tiago B. Rodrigues, **Eva M. Serrao**, **Brett W.C. Kennedy**, **De-en Hu**, **Mikko I. Kettunen**[*], and **Kevin M. Brindle**[*,†]
Cancer Research UK Cambridge Institute, University of Cambridge, Li Ka Shing Centre, Robinson Way, Cambridge, CB2 0RE and Department of Biochemistry, University of Cambridge, Tennis Court Road, Cambridge CB2 1GA, UK

Abstract

Glycolysis in murine lymphoma and lung tumors was monitored by measuring the conversion of hyperpolarized [U-^{2}H, U-^{13}C]glucose to lactate using ^{13}C magnetic resonance spectroscopy and spectroscopic imaging. Labeled lactate was only observed in tumors, and not in surrounding normal tissue or in other tissues in the body, and was markedly decreased at 24 h after treatment with a chemotherapeutic drug. Production of 6-phosphogluconate in the pentose phosphate pathway was also detected. The technique could provide a new way of detecting early evidence of tumor treatment response in the clinic and of monitoring tumor pentose phosphate pathway activity.

Keywords

lactate; treatment response; lymphoma; lung; metabolism

INTRODUCTION

Tumor cells frequently display high rates of aerobic glycolysis [1]. While the hypoxic tumor microenvironment might select for cells that are glycolytic, and thus can generate ATP in the absence of oxygen, it is clear that this and the other metabolic changes observed in tumor cells are driven by oncogene activation and loss of tumor suppressor gene function [2]. Moreover, while these metabolic changes are important for generating ATP under anaerobic conditions, they also have other important functions, such as the generation of metabolic intermediates for biosynthetic pathways [3]. For example glycolytic flux is diverted into the pentose phosphate pathway (PPP) to generate NAPDH for lipid biosynthesis and to combat the increased oxidative load experienced by many tumors [4].

The aberrant metabolism displayed by tumor cells provides opportunities for tumor detection and treatment response monitoring using metabolic imaging [5]. Positron emission tomography (PET) measurements of the uptake and trapping of ^{18}Fluorodeoxyglucose

[†]Corresponding author: Department of Biochemistry, University of Cambridge, Tennis Court Road, Cambridge CB2 1GA, UK. Tel. +44 1223 333674 Fax. +44 1223 766002 kmb1001@cam.ac.uk.
[*]Contributed equally as joint senior authors.

AUTHORS CONTRIBUTIONS T.B.R. and M.I.K. designed the research; T.B.R., E.M.S., B.W.C.K., D.-E.H. and M.I.K. performed the research; T.B.R. and M.I.K. analyzed data; T.B.R., M.I.K., and K.M.B. wrote the paper.

Declaration of competing financial interests The hyperpolarizer is on loan from GE Healthcare and is the subject of a research agreement between the University of Cambridge, Cancer Research UK and GE Healthcare.

Europe PMC Funders Author Manuscripts

(^{18}FDG) have been used to detect tumors and their metastases and decreases in FDG uptake have also been used to detect treatment response in some tumor types [6].

^{13}C magnetic resonance spectroscopy (MRS), which can detect signals from multiple cellular metabolites following administration of a ^{13}C-labelled substrate, including ^{13}C-labelled glucose [7], has been widely used to follow metabolic processes *in vivo*. However, its relatively low sensitivity is a major limitation. The recent development of dynamic nuclear polarization (DNP), which dramatically increases the sensitivity of the ^{13}C MRS experiment (> 10,000 times) [8], has allowed real-time imaging of several substrates and the metabolites formed from them *in vivo* [9]. The most widely used substrate to date has been hyperpolarized [1-^{13}C]pyruvate [10], where decreased label exchange between labeled pyruvate and endogenous lactate in tumors has been shown to be a marker of treatment response [11-13].

The major drawback of the technique is the short half-life of the hyperpolarization, which for [1-^{13}C]pyruvate is ~30 s *in vivo*. This means that imaging must be accomplished with 2–3 min of injection of the polarized material and that its subsequent metabolism should be relatively fast [10]. This would appear to preclude the use of hyperpolarized ^{13}C-labelled glucose, since the glucose carbons have very short T_1s (< 1 s). However deuteration of protonated carbons can significantly extend their T_1s [14]. Previous studies with hyperpolarized [U-^{2}H, U-^{13}C]glucose have shown that hyperpolarized ^{13}C-labeled lactate can be detected in *E. coli* cells [15], yeast [16] and in tumor cells *in vitro* [17]. Hyperpolarized ^{13}C-labeled glucose has been imaged in rats *in vivo* [18], although detection of glucose metabolism was not demonstrated. We show here that injection of hyperpolarized [U-^{2}H, U-^{13}C]glucose allows real-time imaging of glycolytic flux in two murine tumor models *in vivo* and that this flux is decreased in a lymphoma model 24 h after treatment with the chemotherapeutic drug etoposide. We also show that 6-phosphogluconate (6PG), resulting from PPP activity, can be detected. Since hyperpolarized [1-^{13}C]pyruvate has already transferred to the clinic [19], with a study in prostate cancer, the facility to image hyperpolarized glucose and its metabolic product lactate may offer a more sensitive approach for imaging tumor treatment response in the clinic.

RESULTS

Measurements in vivo

Intravenous injection of hyperpolarized [U-^{2}H, U-^{13}C]glucose (100 mM, 0.35 mL) into EL4 tumor-bearing mice (n = 6) resulted in tumor signals from all six ^{13}C nuclei in both anomeric forms (60–100 ppm) (Fig. 1a–b). The polarization decayed with an apparent spin lattice relaxation time, T_1, for the combined resonances, of 8.9 ± 0.6 s (n = 12, average from all animals, pre- and post-treatment) (Fig. 1b). Signal from the labeled C1 carbon of lactate was also observed in the tumor spectra at 15 s post-injection. Lactate detection was not specific to EL4 tumors since similar spectra were obtained from Lewis lung adenocarcinoma tumors (LL2) (Fig. 2a). Labeled lactate was not observed in brain, heart, liver or kidney when the surface coil receiver was placed over these tissues (Fig. 2a), indicating that the lactate signal arises from within the tumor itself, rather than from other tissues via the circulation. A typical ^{13}C chemical-shift image (CSI) acquired at ~15 s after injection of hyperpolarized [U-^{2}H, U-^{13}C]glucose, from an untreated EL4 tumor-bearing mouse (Fig. 2b), showed that the hyperpolarized lactate signal was predominantly within the tumor, consistent with the localized spectra (Fig. 2b). The distribution of lactate in the CSI was similar to that observed after injection of hyperpolarized [1-^{13}C]pyruvate (Fig. 1S, Supplementary Information).

Low levels of dihydroxyacetone phosphate (DHAP), 6PG and bicarbonate (HCO_3^-) were observed in the tumor spectra (Fig. 3). These resonances were assigned on the basis of their

chemical shifts and have been observed previously in experiments with hyperpolarized [U-^{2}H, U-^{13}C]glucose in *E. coli* and yeast [15,16]. 6PG, an intermediate in the PPP, has a similar chemical shift to the glycolytic intermediates, 1,3-biphosphoglycerate (1,3PG), 3-phosphoglycerate (3PG) and 2-phosphoglycerate (2PG). However, we assigned the observed resonance to 6PG since there are only three enzyme-catalyzed steps between glucose and 6PG, as compared to up to eight between glucose and 2PG, and therefore the polarization is more likely to be preserved. Furthermore, although the concentration of DHAP, an upstream intermediate in the glycolytic pathway is greater than those of phosphoglycerates in tumor cells [20], the DHAP signal was comparable to that assigned to 6PG and therefore the contribution from phosphoglycerates is expected to be small.

Flux of ^{13}C label from hyperpolarized [U-^{2}H, U-^{13}C]glucose to lactate was decreased 24 h after treatment of EL4 tumor-bearing animals with etoposide. The lactate/glucose signal ratio was decreased by 62% at 24 h after treatment with etoposide (1.82 ± 0.42% in untreated tumors versus 0.69 ± 0.11% in treated tumors, $P = 0.026$, $n = 6$).

There was no evidence of significant pyruvate oxidation in the TCA cycle in these tumors. In animals injected with hyperpolarized [1-^{13}C]pyruvate (0.2 mL 75 mM i.v.) the $H^{13}CO_3^-$ signal was 0.01 ± 0.006% of the [1-^{13}C]lactate signal ($n = 2$) in slice selective spectra and 0.8 ± 0.1% ($n = 2$) in non-slice selective spectra, where there is some contribution from underlying tissue. Dichloroacetate (150 mg kg^{-1} i.v.) injected 3 min prior to the pyruvate had no significant effect on this ratio.

High-resolution MRS measurements on tumor extracts

The effects of etoposide treatment on the concentrations of unlabeled and ^{13}C-labeled glucose and lactate were determined from high-resolution ^{13}C (Fig. 2S, Supplementary Information) and ^{1}H NMR spectra of EL4 tumor, liver and blood extracts taken from animals at 20 and 150 s after injection of [U-^{13}C]glucose, which was injected at the same concentration as the hyperpolarized [U-^{2}H, U-^{13}C]glucose. Labeled material was distinguished from unlabeled material, where ^{13}C was only present at natural abundance (1.1%), by the presence of ^{13}C-^{13}C spin coupling in the labeled material. The concentrations of unlabeled glucose and lactate determined from the natural abundance ^{13}C signal showed good agreement with the concentrations determined from the ^{1}H NMR spectra (data not shown). There was no detectable labeled lactate in the blood, confirming that the hyperpolarized ^{13}C-labeled lactate observed in the tumor *in vivo* is unlikely to have been washed in from other tissues. Following drug treatment and at 150 s after injection of labeled glucose there was a 50% decrease in the labeled lactate concentration, which was comparable with the 39% decrease in the steady state unlabeled lactate concentration (Table 1; Fig. 2S, Supplementary Information). Flux of labeled glucose into the PPP was assessed by injecting animals with [1,2-^{13}C]glucose and analyzing label incorporation into the 2 and 3 positions of lactate [21]. The ratio of the lactate C3 singlet intensity (from [3-^{13}C]lactate) (corrected for the contribution from background natural abundance signal) to that of the C3 doublet (from [2,3-^{13}C]lactate) was 7 ± 1% ($n = 5$), indicating that flux through the PPP was ~7% of the glycolytic flux, assuming that the singlet arising from lactate C3 is the product of the oxidative branch of the PPP [21]. There was no difference between untreated and treated tumors and in liver the corresponding value was 38 ± 9% ($n = 5$).

DISCUSSION

Previous studies have demonstrated that treatment response can be detected in murine tumor models from the decrease in tumor ^{13}C-labeled lactate concentration in animals injected with ^{13}C-labeled glucose [22,23]. However in these studies, with non-polarized glucose, much higher glucose concentrations were used [2223], the data were acquired for longer periods of

time (80–120 min) and there was insufficient signal for imaging. We have shown here that hyperpolarized [U-^{2}H, U-^{13}C]glucose has a sufficiently long T_1 and degree of polarization to allow detection and imaging of glycolytic flux in murine tumors *in vivo*. Furthermore, the experiment detects tumor treatment response, with a 62% decrease in the lactate/glucose signal ratio at 24 h post treatment of lymphoma tumors with etoposide. This decrease was larger than the 39% decrease in steady state lactate concentration and the 50% decrease in labeled lactate concentration determined from measurements on tumor extracts (Table 1), which may be due, in part, to the slightly higher blood glucose concentration in the drug-treated animals.

Only tumor tissue showed detectable levels of labeled lactate; no signal was detected in brain, heart, liver, or kidney (Fig. 2a) and no labeled lactate was detected in the blood (Table 1). Measurements of labeled lactate concentrations in tumor extracts (Table 1) gave a lactate production rate of ~0.8 μmol min^{-1} g^{-1}, similar to rates reported for other tumor cell types [1] and comparable with the glucose consumption rate measured in rat brain (0.75 μmol min^{-1} g^{-1}) [24] and heart muscle (~1 μmol min^{-1} g^{-1}) [25]. Presumably these tissues showed no signal because of their lower steady state lactate concentrations when compared to tumors [24,25].

The sensitivity of MR detection of hyperpolarized [U-^{2}H, U-^{13}C]glucose and the lactate produced from it is much lower than PET detection of ^{18}FDG and also lower than MR detection of hyperpolarized ^{13}C label exchange between [1-^{13}C]pyruvate and endogenous lactate. The signal-to-noise ratio for the lactate signal produced from hyperpolarized [U-^{2}H, U-^{13}C]glucose was ~10, when the glucose was injected at 0.3 g kg^{-1}, and ~60 when 0.7 g kg^{-1} was injected and an optimized signal acquisition protocol was used, as compared to ~400 for the lactate produced from hyperpolarized [1-^{13}C]pyruvate (injected at ~0.07 g kg^{-1}) [11] (Fig. S1, Supplementary Information). Nevertheless, hyperpolarized [U-^{2}H, U-^{13}C]glucose has some potential advantages for detecting tumor treatment response. Firstly, it does not use ionizing radiation. Secondly, detection of ^{13}C labeled lactate should be advantageous in detecting response in those tumors where ^{18}FDG-PET can show poor contrast, such as brain tumors and in the prostate. Lactate, on the other hand, is much higher in concentration in brain tumors than in the surrounding brain tissue, and the absence of labeled lactate in the kidney in this study indicates that detection of treatment response in prostate cancer should also be possible since there will be little or no labeled lactate in the adjacent bladder.

The polarized pyruvate and ^{18}FDG-PET experiments interrogate only a few steps in glucose metabolism; glucose transport and hexokinase activity in the case of ^{18}FDG-PET and monocarboxylate transporter (MCT) and LDH activities in the case of polarized pyruvate. Whereas, in principle, measurements of hyperpolarized ^{13}C label flux between glucose and lactate can be used to assess flux through the entire glycolytic pathway. This depends on two assumptions. Firstly, that there is unidirectional flux of label from glucose to pyruvate. Since there are three effectively irreversible steps in the glycolytic pathway between glucose and pyruvate, the glycolytic intermediate concentrations are relatively low and there is no measurable gluconeogenic flux, for example we have never detected labeled glucose in in this tumor model in experiments with hyperpolarized [1-^{13}C]pyruvate or [1-^{13}C]lactate[11,26], then this assumption appears justified. Secondly, we assume that most of the hyperpolarized ^{13}C label that reaches pyruvate exchanges into the much larger lactate pool, which has been demonstrated[27], and that little of the pyruvate is oxidized in the mitochondria. Experiments with hyperpolarized [1-^{13}C]pyruvate showed that pyruvate oxidation in the tumor was minimal compared with exchange of ^{13}C label with endogenous lactate, with only 0.01 ± 006% of the hyperpolarized label in lactate appearing in H$^{13}CO_3^-$. In non-slice selective spectra, which include some contribution from underlying tissue, this figure increased to 0.8 ± 0.14%. Dichloroacetate, which has been shown to increase

pyruvate oxidation [28], had no significant effect on this ratio. In a rat brain glioma model the signal from hyperpolarized $H^{13}CO_3^-$ was 4% of that in [1-^{13}C]lactate versus 16% in normal brain [28]. Therefore we conclude that measurements of hyperpolarized ^{13}C label flux between glucose and lactate, in those tissues that have low rates of pyruvate oxidation, such as tumors, can be used to assess net flux through the glycolytic pathway. This measured flux should be sensitive to drugs that inhibit any step in the pathway or which divert flux into other pathways. In principle the polarized pyruvate experiment gives similar information about glycolytic flux since it is sensitive to changes in lactate concentration; increases in lactate concentration resulting in increased label exchange [11]. However, this need not be the case. In human breast cancer cells (MCF7) treated with a MEK inhibitor there was decreased lactate labeling despite an increase in lactate concentration. The increased lactate concentration was attributed to an increase in glycolytic flux and the decreased labeling due to inhibition of the MCTs [29]. Another advantage of the polarized glucose experiment is that glucose can be used at physiological concentrations whereas pyruvate is used at supra physiological concentrations. In the first clinical trial of hyperpolarized [1-^{13}C]pyruvate, pyruvate was injected at 0.43 mL kg^{-1} of a 250 mM solution (Clinical-Trials.gov Identifier: NCT01229618), which equates to a whole blood concentration of ~1.5 mM, whereas the physiological concentration is ~0.060 mM. In clinical intravenous glucose tolerance tests glucose is injected at up to 0.5 g kg^{-1}, which equates to a whole blood concentration of ~40 mM.

The production of $^{13}CO_2$ in the irreversible oxidative decarboxylation catalyzed by 6-phosphogluconate dehydrogenase potentially provides a measure of net flux into the PPP. Measurements with [1,2-^{13}C]glucose showed that ~7% of labeled lactate was produced via the PPP, which is comparable with a measured hyperpolarized $H^{13}CO_3^-$/6-phosphogluconate $^{13}C_1$ ratio of ~10%. However this measurement may be compromised if there is significant $^{13}CO_2$ production resulting from pyruvate decarboxylation in the reaction catalyzed by pyruvate dehydrogenase. In non-slice selective spectra in animals injected with hyperpolarized [1-^{13}C]pyruvate the hyperpolarized $H^{13}CO_3^-$ signal was 0.8% of the [1-^{13}C]lactate signal as compared with ~2% in animals injected with hyperpolarized [U-^{2}H, U-^{13}C]glucose. Since flux into the pathway is controlled by glucose 6-phosphate dehydrogenase activity [30] labeling of 6PG may provide a more reliable measure of PPP flux.

The major limitation of using hyperpolarized [U-^{2}H, U-^{13}C]glucose is the short polarization lifetime. Reducing the degree of ^{13}C substitution in the molecule, and thus homonuclear dipolar relaxation, will extend the lifetime, although the effect is relatively small. The T_1s for the C4 carbons in the α and β anomers of [U-^{2}H, U-^{13}C]glucose were increased by ~30% in the natural abundance C4 carbons in [U-^{2}H]glucose. Using [U-^{2}H, 3,4-$^{13}C_2$] or [U-^{2}H, 3-^{13}C]glucose would have the added advantages that they produce [1-^{13}C]lactate, if metabolized via the glycolytic pathway, which would improve detection since the lactate resonance will be a singlet, and could also provide another assessment of PPP activity since they should also produce [1,2-^{13}C]lactate if metabolized via the PPP. Sensitivity could also be improved by increasing the level of polarization (from the ~15% achieved here) and by injecting higher glucose concentrations, although this may only be possible in pre-clinical studies.

ONLINE METHODS

Cell culture

Murine T-cell lymphoma (EL4) and Lewis lung carcinoma (LL2) cells were from the American Type Culture Collection (ATCC). EL4 cells were grown to a maximum cell density of ~5 × 10^7 cells mL^{-1} in RPMI 1640 medium (Invitrogen) supplemented with 2 mM L-glutamine and 10% FCS (fetal calf serum, PAA Laboratories). LL2 cells were grown

in DMEM (Invitrogen) supplemented with 4.5 mg mL^{-1} glucose, 2 mM L-glutamine, and 10% FBS (fetal bovine serum, PAA laboratories).

Animal preparation

Experiments were conducted in compliance with project and personal licenses issued under the Animals (Scientific Procedures) Act of 1986 and were designed with reference to the U.K. Co-ordinating Committee on Cancer Research guidelines for the welfare of animals in experimental neoplasia. A local ethical review committee approved the work.

EL4 cells (5×10^6) were resuspended in ice-cold PBS and implanted into female C57BL/6 mice (n = 40, 6–8 weeks of age; Charles River Ltd.) by subcutaneous injection, in the lower flank. LL2 cells were implanted (6×10^6) in a single animal. At this location there was no detectable respiratory motion in MR images. MRS was performed when the tumors had grown to a size of ~2 cm^3, which for EL4 tumors was typically 10 d following implantation. Animals were imaged before and 24 h after treatment with 67 mg etoposide kg^{-1} body weight (Eposin, 20 mg mL; PCH Pharmachemie) and were anaesthetized by inhalation of 1–2% isoflurane (Isoflo, Abbotts Laboratories Ltd.) in air/O_2 (75/25%, 2 L min^{-1}) and body temperature maintained by blowing warm air through the magnet bore. Breathing rate (~80 bpm) and body temperature (37 °C) were monitored during experiments (Biotrig). Hyperpolarized agents were injected intravenously via a tail vein catheter.

Perchloric acid extracts from untreated (n = 15) and etoposide-treated (n = 14) EL4 tumor-bearing mice were prepared following injection of 0.35 mL 100 mM [U-^{13}C]glucose. Protonated glucose was used to avoid the complex multiplets arising from ^{13}C- ^{2}H coupling. The mice were killed by cervical dislocation after either 20 s (n = 5, treated; n = 5, untreated) or 150 s (n = 4, treated; n = 4, untreated), and the tumors and livers were rapidly freeze-clamped in liquid nitrogen-cooled tongs. Another cohort was similarly prepared (n = 3, untreated; n = 3, etoposide-treated) and blood was obtained by cardiac puncture after 20 s. A third cohort were killed by cervical dislocation 150 s after injection with 0.35 mL of 100 mM [1,2-^{13}C]glucose (n = 3, treated; n = 2, untreated) and the tumors and livers rapidly freeze-clamped. Perchloric acid extracts were prepared using 7% perchloric acid (1:8 w/v), which were then neutralized with KOH, lyophilized, and dissolved in 99.9% deuterium oxide.

Hyperpolarization of [U-^{2}H, U-^{13}C]glucose

For therapy response studies in EL4 tumors and acquisition of ^{13}C MR spectra from LL2 tumors, brain, heart, liver, and kidneys, trityl radical (25.8 mM, OX063; GE Healthcare), gadolinium chelate (2.6 mM, Dotarem; Guerbet) and [U-^{2}H, U-^{13}C]glucose (3.55 M; Cambridge Isotopes) were dissolved in 50 μl deuterium oxide. Deuterated DMSO (25 μl) was added to ensure glass formation in the solid state. For the remaining experiments, the glucose preparation was modified slightly (25.8 mM trityl radical, 1.3 mM gadolinium chelate and 3.55 M [U-^{2}H, U-^{13}C]glucose were dissolved in 130 μl deuterium oxide). Samples were polarized using a Hypersense polarizer (Oxford Instruments) for 120 min before dissolution at 180 °C with 3 mL of deuterated saline to yield 100 mM and 200 mM final glucose concentrations, respectively. The samples were cooled to ~37 °C before intravenous injection. The polarization levels were ~15% at the time of dissolution.

Hyperpolarization of [1-^{13}C]pyruvate

[1-^{13}C]pyruvic acid (43.5 mg) (Sigma-Aldrich Company Ltd.), 0.7 mg of trityl radical OX063 and 1.2 mg of 1:10 gadolinium chelate solution were placed in the hyperpolarizer. The frozen sample was irradiated for 1 h and then dissolved in a solution containing 100 mg

L^{-1} ethylenediaminetetraacetic acid (EDTA), 30 mM NaCl, 94 mM NaOH and 40 mM 4-(2-hydroxyethyl)-1-piperazineethanesulfonic acid (HEPES) in D_2O at ~180°C and ~1 MPa.

Magnetic resonance imaging and spectroscopy in vivo

Experiments were performed in a 7.0-T horizontal bore magnet (Varian) using an actively decoupled dual-tuned $^{13}C/^{1}H$ volume transmit coil (Rapid Biomedical,) and a 20-mm ^{13}C receiver surface coil (Rapid Biomedical) placed over the tissue of interest. Hyperpolarized [U-^{2}H, U-^{13}C]glucose (0.35 mL 100 mM, or 0.4 mL 200 mM; the dead volume of injection line was ~50 μl) was injected intravenously over a period of 3 s and the animal placed inside the magnet. Data acquisition was started 15 s after the start of injection, with a total time between dissolution and data acquisition of ~30 s. A series of frequency-selective ^{13}C spectra were collected, with four spectra collected from the lactate region (1 ms sinc pulse with flip angle 20°) followed by one spectrum collected from the glucose region (flip angle 10°) and the sequence repeated over a period of 40 s. The spectral width was 4 kHz collected into 768 complex points, the repetition time was 0.2 s and echo time 0.8 ms. In two animals, 9 lactate spectra were acquired followed by 1 glucose spectrum with a flip angle of 10° (0.75 ms sinc pulse), a repetition time of 0.1 s, echo time of 0.45 ms and a spectral width of 6 kHz. In three animals, two ^{13}C chemical shift selective images were collected (field of view 32 × 32 mm, repetition time 30 ms, echo time 0.8 ms, spectral width 6 kHz, data matrix 16 × 16, flip angle 5 degrees); the first from the glucose resonance (15 s post injection) and second from the lactate resonance (25 s post injection). A urea phantom was included for reference. An identical chemical shift selective image was acquired in the same animals 25 s after injection of hyperpolarized pyruvate. Data were overlaid on ^{1}H spin-echo reference images (field of view 32 × 32 mm, data matrix 128 × 128, repetition time 1.8 s, echo time 20 ms, slice thickness 2 mm).

Lactate and glucose spectra were summed separately and phase- and baseline-corrected, using Matlab (MathWorks). Spectra were referenced to the glucose C1 carbon at 98.66 p.p.m. Ratios of the lactate (183–187 p.p.m.) and glucose (60–100 p.p.m.) peak integrals, summed over the whole time course, were calculated. The signals were not corrected for the different number of ^{13}C nuclei in glucose (6) and lactate (1) nor for differences in flip angle. For comparison the summed first second of data acquisition (four lactate spectra, one glucose spectrum) were also analyzed and similar results were obtained. For determination of the apparent glucose T_1, signal integrals were fitted to a mono-exponential decay function. In order to account for possible polarization variations at the time of glucose injection, spectra were normalized using the initial glucose signal intensity.

For experiments with [1-^{13}C]pyruvate 0.2 mL of the hyperpolarized solution (75 mM) was injected i.v. and data acquisition started at 15 s post-injection. A series of alternating slice-selective and non-slice selective spectra were collected with 100 ms between spectra, using the same acquisition conditions as used for the glucose experiments. The imaging slice was selected through tumor. For some experiments dichloroacetate (150 mg kg^{-1}) was injected i.v. 3 min before the hyperpolarized pyruvate.

High-resolution ^{13}C and ^{1}H NMR spectroscopy

High-resolution ^{1}H and ^{1}H-decoupled ^{13}C NMR spectra of tumor, liver and whole blood extracts were obtained at 14.1 T (25 °C, pH 7.2) using a Bruker 600 MHz NMR spectrometer (Bruker) using a 5-mm probe. The acquisition conditions were: ^{1}H, 90° pulses; 7.3 kHz spectral width; 4.5 s acquisition time; 32k data points; 64 transients; and 12.5 s recycling time; ^{13}C, 30° pulses; 36.0 kHz spectral width; 0.9 s acquisition time; 32k data points; 2048 transients; and 14 s recycling time. Chemical shifts were referenced to 3-(trimethylsilyl)-2,2′,3,3′-tetradeuteropropionic acid (TSP, 0.0 p.p.m.). Spectral

deconvolution and multiplet structures were analyzed using the PC-based (Intel Centrino Platform) NMR program, ACDSpecManager (ACD/Labs). Data were zero-filled twice and multiplied by an exponential function prior to Fourier transformation. All NMR resonance areas were normalized relative to the 5 mM TSP resonance integral. For reference purposes, a high-resolution ^{13}C NMR spectrum was acquired from a [U-^{2}H, U-^{13}C]glucose solution, using the same acquisition parameters as described above (Fig. 1a).

Statistical analysis

Results are expressed as mean ± S.E.M. unless stated otherwise. Statistical significance was tested using Excel (Microsoft) with a two-tailed Student's *t*-test.

Supplementary Material

Refer to Web version on PubMed Central for supplementary material.

Acknowledgments

The work was supported by a Cancer Research UK Programme grant (C197/A3514) and by a Translational Research Program Award from The Leukemia & Lymphoma Society to K.M.B.. T.B.R. was in receipt of an Intra-European Marie Curie (FP7-PEOPLE-2009-IEF, Imaging Lymphoma) and a Long-term EMBO (EMBO-ALT-1145-2009) fellowships. E.M.S. was a recipient of a fellowship from the European Union Seventh Framework Programme (FP7/2007-2013) under the Marie Curie Initial Training Network *METAFLUX* (project number 264780). E.M.S. acknowledges the educational support of Programme for Advanced Medical Education from Calouste Gulbenkian Foundation, Champalimaud Foundation, Ministerio de Saude and Fundacao para a Ciencia e Tecnologia, Portugal. The polarizer and related materials were provided by GE-Healthcare. The authors thank Ferdia Gallagher for help with the polarizer. This is a contribution from Cambridge – Manchester Cancer Imaging Centre, which is funded by the EPSRC and Cancer Research UK.

REFERENCES

1. Gatenby RA, Gillies RJ. Why do cancers have high aerobic glycolysis? Nature Rev Cancer. 2004; 4:891–899. [PubMed: 15516961]
2. Hsu PP, Sabatini DM. Cancer cell metabolism: Warburg and beyond. Cell. 2008; 134:703–707. [PubMed: 18775299]
3. Vander Heiden MG, Cantley LC, Thompson CB. Understanding the Warburg Effect: The Metabolic Requirements of Cell Proliferation. Science. 2009; 324:1029–1033. [PubMed: 19460998]
4. Cairns RA, Harris IS, Mak TW. Regulation of cancer cell metabolism. Nature Rev Cancer. 2011; 11:85–95. [PubMed: 21258394]
5. Brindle K. New approaches for imaging tumour responses to treatment. Nature Rev Cancer. 2008; 8:94–107. [PubMed: 18202697]
6. Weber W. Use of PET for monitoring cancer therapy and for predicting outcome. J Nucl Med. 2005; 46:983–995. [PubMed: 15937310]
7. Mason GF, et al. Simultaneous determination of the rates of the TCA cycle, glucose-utilization, alpha-ketoglutarate glutamate exchange, and glutamine synthesis in human brain by NMR. J Cereb Blood Flow Metab. 1995; 15:12–25. [PubMed: 7798329]
8. Ardenkjaer-Larsen JH, et al. Increase in signal-to-noise ratio of > 10,000 times in liquid-state NMR. Proc Natl Acad Sci U S A. 2003; 100:10158–10163. [PubMed: 12930897]
9. Kurhanewicz J, et al. Analysis of cancer metabolism by imaging hyperpolarized nuclei: Prospects for translation to clinical research. Neoplasia. 2011; 13:81–97. [PubMed: 21403835]
10. Brindle KM, Bohndiek SE, Gallagher FA, Kettunen MI. Tumor imaging using hyperpolarized ^{13}C magnetic resonance spectroscopy. Magn Reson Med. 2011; 66:505–519. [PubMed: 21661043]
11. Day SE, et al. Detecting tumor response to treatment using hyperpolarized ^{13}C magnetic resonance imaging and spectroscopy. Nature Med. 2007; 13:1382–1387. [PubMed: 17965722]

12. Ward CS, et al. Noninvasive detection of target modulation following phosphatidylinositol 3-kinase inhibition using hyperpolarized ^{13}C magnetic resonance spectroscopy. Cancer Res. 2010; 70:1296–1305. [PubMed: 20145128]
13. Witney TH, Kettunen MI, Brindle KM. Kinetic modeling of hyperpolarized ^{13}C label exchange between pyruvate and lactate in tumor cells. J Biol Chem. 2011; 286:24572–24580. [PubMed: 21596745]
14. Allouche-Arnon H, Lerche MH, Karlsson M, Lenkinski RE, Katz-Brull R. Deuteration of a molecular probe for DNP hyperpolarization – a new approach and validation for choline chloride. Contrast Media Mol Imaging. 2011; 6:499–506. [PubMed: 22144028]
15. Meier S, Jensen PR, Duus JØ. Real-time detection of central carbon metabolism in living Escherichia coli and its response to perturbations. FEBS Lett. 2011; 585:3133–3138. [PubMed: 21907715]
16. Meier S, Karlsson M, Jensen PR, Lerche MH, Duus JO. Metabolic pathway visualization in living yeast by DNP-NMR. Mol Biosystems. 2011; 7:2834–2836.
17. Harris T, Frydman L, Degani H. Metabolism of hyperpolarized U-^{13}C-d$_7$-D-Glucose in living breast cancer cell cultures. Proc Intl Soc Mag Reson Med. 2011; Vol. 19:63.
18. Allouche-Arnon H, et al. *In vivo* magnetic resonance imaging of glucose – initial experience. Contrast Media Mol Imaging. 2013; 8:72–82. [PubMed: 23109395]
19. Nelson S, et al. Proof of concept clinical trial of hyperpolarized C-13 pyruvate in patients with prostate cancer. Proc Intl Soc Magn Reson Med. 2012; Vol. 20:274.
20. Gumaa KA, McLean P. The pentose phosphate pathway of glucose metabolism. Biochemical Journal. 1969; 115:1009–1029. [PubMed: 5360673]
21. Marin-Valencia I, et al. Glucose metabolism via the pentose phosphate pathway, glycolysis and Krebs cycle in an orthotopic mouse model of human brain tumors. NMR Biomed. 2012; 25:1177–1186. [PubMed: 22383401]
22. Rivenzon-Segal D, Margalit R, Degani H. Glycolysis as a metabolic marker in orthotopic breast cancer, monitored by in vivo C-13 MRS. Am J Physiol Endocrinol Metab. 2002; 283:E623–E630. [PubMed: 12217878]
23. Poptani H, et al. Cyclophosphamide treatment modifies tumor oxygenation and glycolytic rates of RIF-1 tumors: C-13 magnetic resonance spectroscopy, Eppendorf electrode, and redox scanning. Cancer Res. 2003; 63:8813–8820. [PubMed: 14695197]
24. Madsen PL, Cruz NF, Sokoloff L, Dienel GA. Cerebral oxygen/glucose ratio is low during sensory stimulation and rises above normal during recovery: Excess glucose consumption during stimulation is not accounted for by lactate efflux from or accumulation in brain tissue. J Cereb Blood Flow Metab. 1999; 19:393–400. [PubMed: 10197509]
25. Neely JR, Whitmer JT, Rovetto MJ. Effect of coronary blood-flow on glycolytic flux and intracellular pH in isolated rat hearts. Circ Res. 1975; 37:733–741. [PubMed: 156]
26. Kennedy BWC, Kettunen MI, Hu D-E, Brindle KM. Probing lactate dehydrogenase activity in tumors by measuring hydrogen/deuterium exchange in hyperpolarized L-[1-^{13}C,U-^{2}H]Lactate. J Am Chem Soc. 2012; 134:4969–4977. [PubMed: 22316419]
27. Kettunen MI, et al. Magnetization transfer measurements of exchange between hyperpolarized [1-^{13}C]pyruvate and [1-^{13}C]lactate in a murine lymphoma. Magn Reson Med. 2010; 63:872–880. [PubMed: 20373388]
28. Park JM, et al. Metabolic response of glioma to dichloroacetate measured in vivo by hyperpolarized ^{13}C magnetic resonance spectroscopic imaging. Neuro-Oncology. 2013; 15:433–441. [PubMed: 23328814]
29. Lodi A, Woods SM, Ronen SM. Treatment with the MEK inhibitor U0126 induces decreased hyperpolarized pyruvate to lactate conversion in breast, but not prostate, cancer cells. NMR Biomed. 2013; 26:299–306. [PubMed: 22945392]
30. Riganti C, Gazzano E, Polimeni M, Aldieri E, Ghigo D. The pentose phosphate pathway: An antioxidant defense and a crossroad in tumor cell fate. Free Radic Biol Med. 2012; 53:421–436. [PubMed: 22580150]

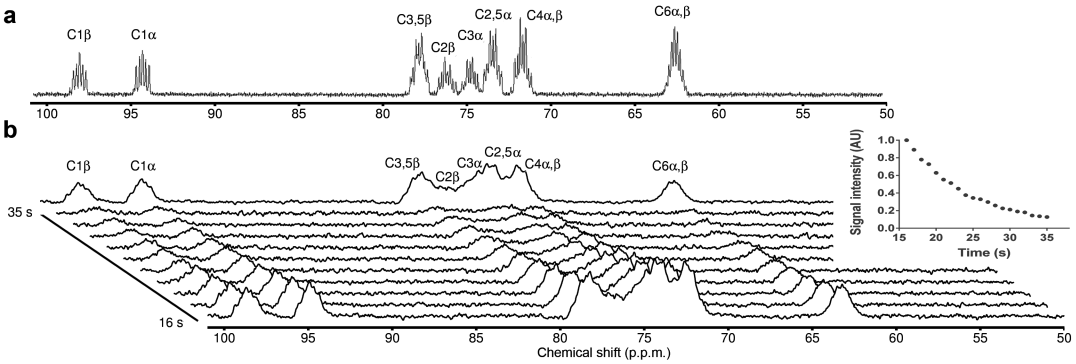

Figure 1. [U-^{2}H, U-^{13}C]glucose signals are detectable *in vivo*

(a) ^{13}C NMR spectrum of [U-^{2}H, U-^{13}C]glucose *in vitro*. The resonance at 65 p.p.m. is from glucose C6 α,β; the resonances between 72–79 p.p.m. are from glucose C2–5 α,β; and the resonances at 94 and 98 p.p.m. are from glucose C1α and C1β, respectively. All the resonances are split into multiplets due to *J*-coupling between ^{13}C-^{13}C and ^{13}C-^{2}H. **(b)** Representative ^{13}C tumor spectra acquired between 16 s and 36 s after the intravenous injection of 0.35 mL 100 mM hyperpolarized [U-^{2}H, U-^{13}C]glucose. For clarity, only every other time point is shown. The top spectrum in the stacked plot is the sum of the first 20 s of data acquisition. The [U-^{2}H, U-^{13}C]glucose signals in the tumor decay with an apparent spinlattice relaxation time, T_1, of ~9 s. AU, arbitrary units.

Europe PMC Funders Author Manuscripts

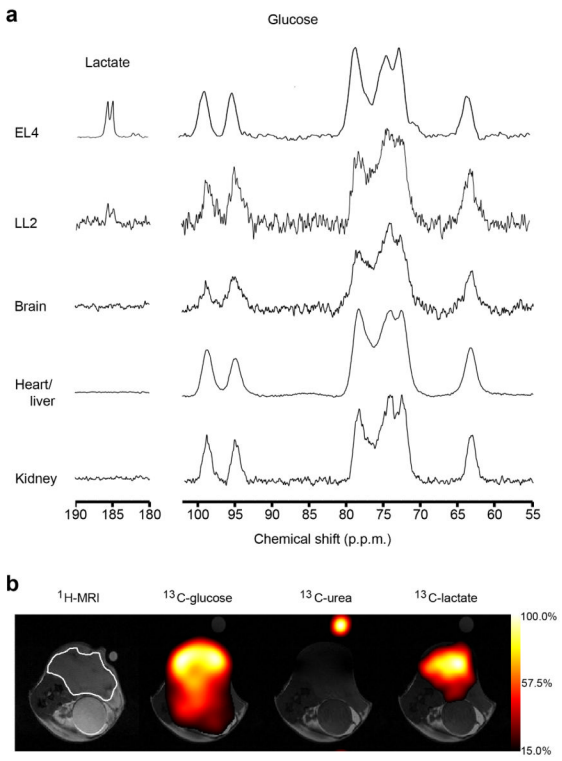

Figure 2. ^{13}C spectroscopic imaging showing the spatial distribution of labeled glucose and lactate

(a) Representative ^{13}C MR spectra acquired from subcutaneous EL4 and LL2 tumors, brain, heart, liver, and kidneys 15 s after the injection of 0.35 mL 100 mM hyperpolarized [U-^{2}H, U-^{13}C]glucose. The lactate spectra are the sum of 4 transients collected over a period of 1 s, whereas a single transient was acquired for the glucose spectra. Flux of hyperpolarized ^{13}C label was only observed between [U-^{2}H, U-^{13}C]glucose (63–99 p.p.m.) and lactate C1 (doublet at ~185 p.p.m.) in EL4 and LL2 tumors. **(b)** Representative chemical shift selective images obtained ~15 s after intravenous injection of 0.4 mL 200 mM hyperpolarized [U-^{2}H, U-^{13}C]glucose into an EL4 tumor-bearing mouse. The spatial distribution of glucose, urea and lactate are displayed as voxel intensities relative to their respective maxima. The ^{1}H MR images, shown in gray scale, were used to define the anatomical location of the tumor (outlined in white). A urea phantom was included to serve as a reference. The color scales represent arbitrary linearly distributed intensities for the hyperpolarized images.

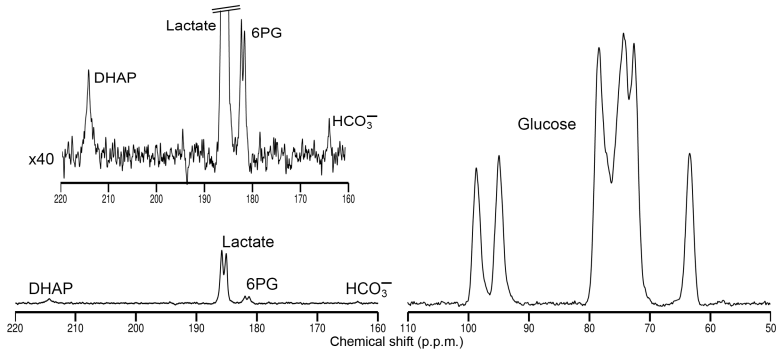

Figure 3. ^{13}C MR spectrum from an untreated subcutaneous EL4 lymphoma tumor

The spectrum is the sum of 54 transients acquired over a period of 6 s, ~15 s after intravenous injection of 0.4 mL 200 mM hyperpolarized [U-^{2}H, U-^{13}C]glucose. The small difference in signal-to-noise ratios between the glucose and lactate regions of the summed spectrum is the result of interleaved signal acquisition from the glucose and lactate regions, with more sampling of the lactate region (see Methods). The inset shows a ×40 magnification of the 160–220 p.p.m. region. This shows bicarbonate C1 (~164 p.p.m., HCO_3^-), 6-phosphogluconate C1 (~182 p.p.m., 6PG), lactate C1 (~185 p.p.m.) and dihydroxyacetone phosphate C2 (~214 p.p.m., DHAP). The signals from hyperpolarized [U-^{2}H, U-^{13}C]glucose are located between 63 and 99 p.p.m..

Table 1

Glucose and lactate concentrations measured in tissue extracts.

		Natural abundance signals		[U-^{13}C]Glucose signals	
		Glucose	**Lactate**	**Glucose**	**Lactate**
		20 s post-injection			
EL4 (μmol g^{-1} wt)	**Untreated**	0.42±0.06	20.7±3.0	0.13±0.02	0.49±0.10
	Treated	0.46±0.13	12.7±1.9[a]	0.16±0.04	0.50±0.13
Blood (μmol mL^{-1})	**Untreated**	3.3±0.1	3.3±0.4	1.8±0.1	n.d.
	Treated	3.2±1.0	3.3±0.6	3.8±0.9	n.d.
Liver (μmol g^{-1} wt)	**Untreated**	11.4±1.1	7.2±1.3	1.7±0.4	0.20±0.06
	Treated	10.6±1.5	5.4±0.6	1.4±0.3	0.06±0.02 [a]
		150 s post-injection			
EL4 **(μmol g^{-1} wt)**	**Untreated**	1.4±0.3	20.0±1.0	0.40±0.07	1.9±0.4
	Treated	1.5±0.3	12.0±0.5 [a]	0.49±0.10	1.2±0.2
Liver (μmol g^{-1} wt)	**Untreated**	9.2±3.2	6.0±0.3	1.1±0.1	0.31±0.01
	Treated	9.8±3.0	5.3±0.7	1.3±0.2	0.29±0.04

Tumors were freeze-clamped and extracted 20 s or 150 s after intravenous injection of 0.35 mL 100 mM [U-^{13}C]glucose. n = 5 for EL4 and liver samples (post 20 s) and n = 4 for EL4 and liver samples (post 150 s), n = 3 for blood plasma samples. Mean ± S.E.M.;

[a] $p < 0.05$; n.d., not detected.